Available online at www.sciencedirect.com
ScienceDirect
Polymer 47 (2006) 7572–7579
polymer
www.elsevier.com/locate/polymer

Small-angle neutron scattering study on block and gradient copolymer aqueous solutions

Satoshi Okabe [a], Ken-ichi Seno [b], Shokyoku Kanaoka [b], Sadahito Aoshima [b], Mitsuhiro Shibayama [a,*]

[a] *Neutron Science Laboratory, Institute for Solid State Physics, The University of Tokyo, Kashiwanoha, Kashiwa, Chiba 277-8581, Japan*
[b] *Department of Macromolecular Science, Graduate School of Science, Osaka University, Toyonaka, Osaka 560-0043, Japan*

Received 15 June 2006; received in revised form 7 August 2006; accepted 20 August 2006
Available online 8 September 2006

Abstract

The small-angle neutron scattering investigation was carried out on semi-dilute aqueous solutions of block and gradient copolymers comprising pEOVE and pMOVE, $pEOVE_{300}$-*block*-$pMOVE_{300}$ (Block) and p(EOVE-*grad*-MOVE)$_{600}$ (Grad). Here, pEOVE and pMOVE denote poly(2-ethoxyethyl vinyl ether) and poly(2-methoxyethyl vinyl ether), respectively, and the numbers indicate the degrees of polymerization. The monomer composition in the Grad had a gradient along the polymer chain. For 20.0 wt% solutions, a microphase-separated structure and physical gelation were observed both in Block and in Grad systems. In the case of the Grad system, a gradual microphase separation took place as a function of temperature via a micellization with a small radius of core, characterized by the ''reel-in'' process, i.e., a winding of polymer chains to the core of a micelle because of the gradient composition. On the other hand, the Block system underwent a stepwise transition with respect to temperature. The relationship between microphase separation and the rheological behavior is explained from the viewpoint of microscopic structure.

Keywords: Gradient copolymer; Small-angle neutron scattering; Microphase separation

1. Introduction

Block copolymers have been widely investigated because of their unique chemical structure, i.e., a polymer consisting of unlike polymer chains chemically bonded to each other [1–3]. One of the unique features of block copolymer systems is the capability of microphase separation, i.e., a phase separation of order of the size of the block copolymer. A variety of morphologies in microphase-separated structures have been reported so far. It is needless to mention that the uniqueness of the physical properties of block copolymers is ascribed to the chemical bonding that connects the constituent block chains at which the chemical composition changes stepwise. It is naively expected what happens if the change in the composition has a gradient. Hashimoto and coworkers prepared two types of ''tapered'' block copolymers and investigated their microdomain structures and mechanical properties. They reported the presence of two types of mixing depending on the structure, namely ''domain boundary mixing'' and ''mixing-in domain'' [4]. The former is a mixing of A and B segments locally at the interface, while in the latter case a mixing occurs in each domain due to the random sequence of A and B segments in a chain. However, the chemical composition gradient could not be well controlled because of difficulty in anionic polymerization.

Theoretical investigations have been made to elucidate the nature of two-component polymeric systems having a gradient composition. Lefebvre et al. predicted that a gradient copolymer is less favorable in phase separation and the size of

* Corresponding author. Tel.: +81 4 7136 3418; fax: +81 4 7134 6069.
E-mail address: shibayama@issp.u-tokyo.ac.jp (M. Shibayama).

0032-3861/$ - see front matter © 2006 Elsevier Ltd. All rights reserved.
doi:10.1016/j.polymer.2006.08.045

microphase separation is smaller than the corresponding block copolymers [5]. They also addressed that such microphase separation would hardly occur in bulk. On the other hand, possibility of a novel type microphase separation in gradient copolymer different from that in block copolymer was theoretically shown by Aksimentiev and Holyst [6].

Recently, Aoshima et al. succeeded in preparing copolymers having a variety of chemical architectures, such as graft, star copolymers [7]. Since living cationic polymerization is employed, the molecular weight and its distribution can be easily controlled. In addition, the living polymerization allows one to choose the second (or third, …) monomers to be attached on. These copolymers commonly carry oxyethylene groups in the side chain, leading to water-solubility. Among a large number of applications of this technique, gradient copolymers have also been prepared [8]. In the previous paper, we carried out structural investigation of a gradient copolymer in a dilute aqueous solution, p(EOVE-*grad*-MOVE)$_{600}$ (Grad) and pEOVE$_{300}$-*block*-pMOVE$_{300}$ (Block) in water [9]. Here, pEOVE and pMOVE denote poly(2-ethoxyethyl vinyl ether) and poly(2-methoxyethyl vinyl ether), respectively, and the numbers indicate the degrees of polymerization. An interesting micelle formation mechanism, called ''reel-in'' effect, was observed, and its structure was extensively investigated.

In the present paper, we report the microdomain structures and their formation mechanism of the gradient copolymer aqueous systems on the basis of the small-angle neutron scattering (SANS) data as a function of temperature, T. It will be shown that the ''reel-in'' effect plays a key role in microphase separation. The mechanism of microphase separation in the Grad system will be compared with that of the Block system.

2. Experimental section

2.1. Samples

p(EOVE-*grad*-MOVE)$_{600}$ (Grad) and pEOVE$_{300}$-*block*-pMOVE$_{300}$ (Block) were prepared by living cationic polymerization. The details of polymer preparation are described elsewhere [9]. Fig. 1 schematically shows the chemical structure of Block and Grad. The number of EOVE and MOVE monomer units in a polymer chain is about 300 both for Block and Grad. The observed ''instantaneous'' composition of MOVE in a Grad polymer is also shown as open circles in Fig. 1, which is in accord with the theoretical curve (broken line) [9,10]. On the other hand, the solid line shows the instantaneous composition of MOVE in Block.

For SANS experiments, deuterated water (D_2O) was used instead of protonated water as the solvent in order to enhance the scattering contrast. The 0.3 wt% aqueous solutions of Block and Grad were coded as Block03 and Grad03, and 20 wt% solutions as Block20 and Grad20, respectively. It should be noted here that aqueous solutions of pEOVE homopolymer has a precipitation point, i.e., LCST at around 20 °C [11,12].

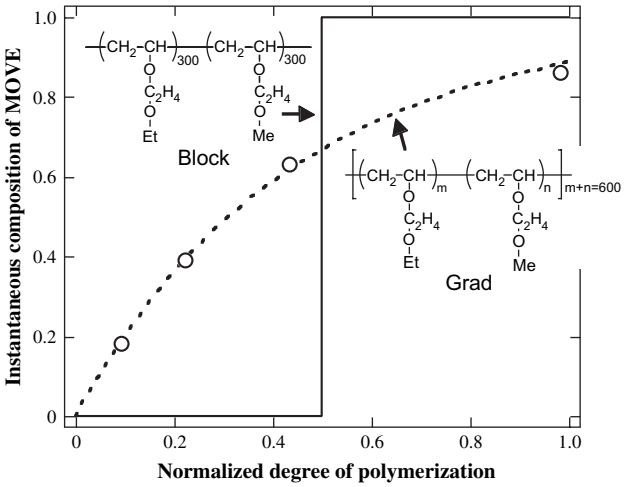

Fig. 1. The chemical schemes of the block (Block) and gradient (Grad) copolymers. The open circles and the broken line show the observed and calculated instantaneous compositions of MOVE, respectively.

2.2. Rheological measurements

The dynamic viscoelasticity of the polymer solutions was measured with a stress controlled rheometer (DAR-100, Reologica) equipped with a cone-and-plate geometry with a diameter of 40 mm and a cone angle of 4°. The values of the stress amplitude were monitored to ensure that all dynamic experiments were performed within the linear viscoelastic regime, in which the dynamic storage modulus (G') and loss modulus (G'') were independent of the applied stress. The dynamic viscoelastic measurement was conducted at various temperatures (10–60 °C) with a frequency of 1.0 Hz.

2.3. Small-angle neutron scattering (SANS)

SANS experiments were carried out at the SANS-U instrument, the Institute for Solid State Physics, the University of Tokyo, Tokai, Japan [13]. The wavelength of the incident neutrons was monochromatized with a mechanical velocity selector to be 0.70 nm with a distribution of ca. 10% in FWHM. Each sample was loaded in a quartz cell of 1.00 mm thickness and was irradiated by the neutron beam having the cross section of 5.0 mm in diameter for 3–120 min depending on the scattering intensity. The scattered neutrons were counted with a two-dimensional area detector and the scattering intensity was circularly averaged and then corrected for transmission and for the cell scattering. The subsequent absolute scattering intensity calibration was carried out with the incoherent scattering from a polyethylene of secondary standard [14].

3. Results and discussion

3.1. Rheological measurements

Fig. 2 shows temperature variations of the storage (G') and loss moduli (G'') of 20 wt% aqueous solutions of (a) Block (Block20) and (b) Grad (Grad20). In the case of Block20, sharp

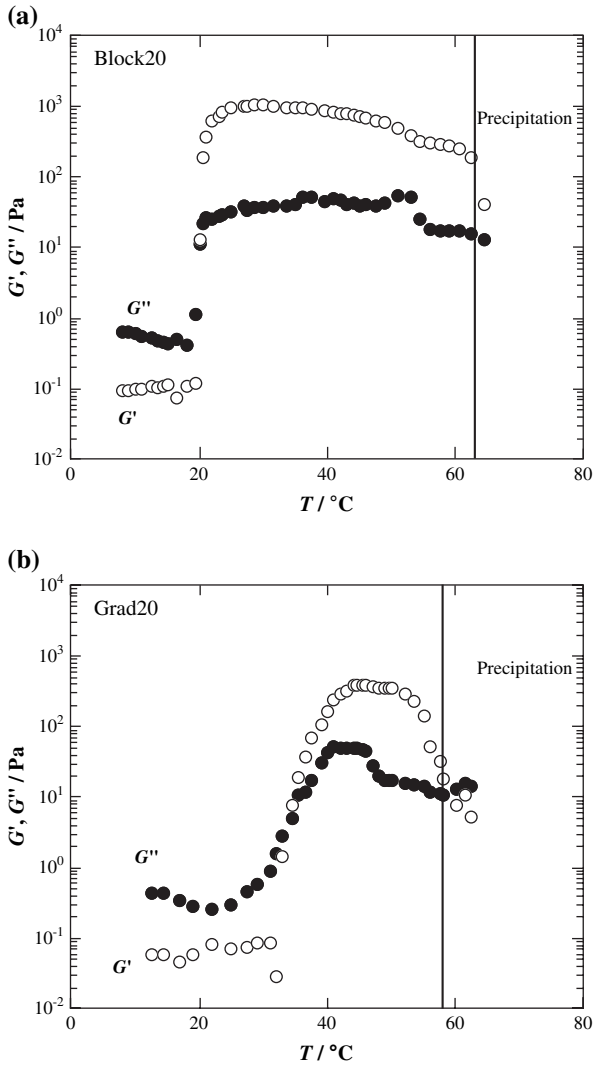

Fig. 2. Temperature variations of storage (G') and loss (G'') moduli (a) in Block20 and (b) in Grad20.

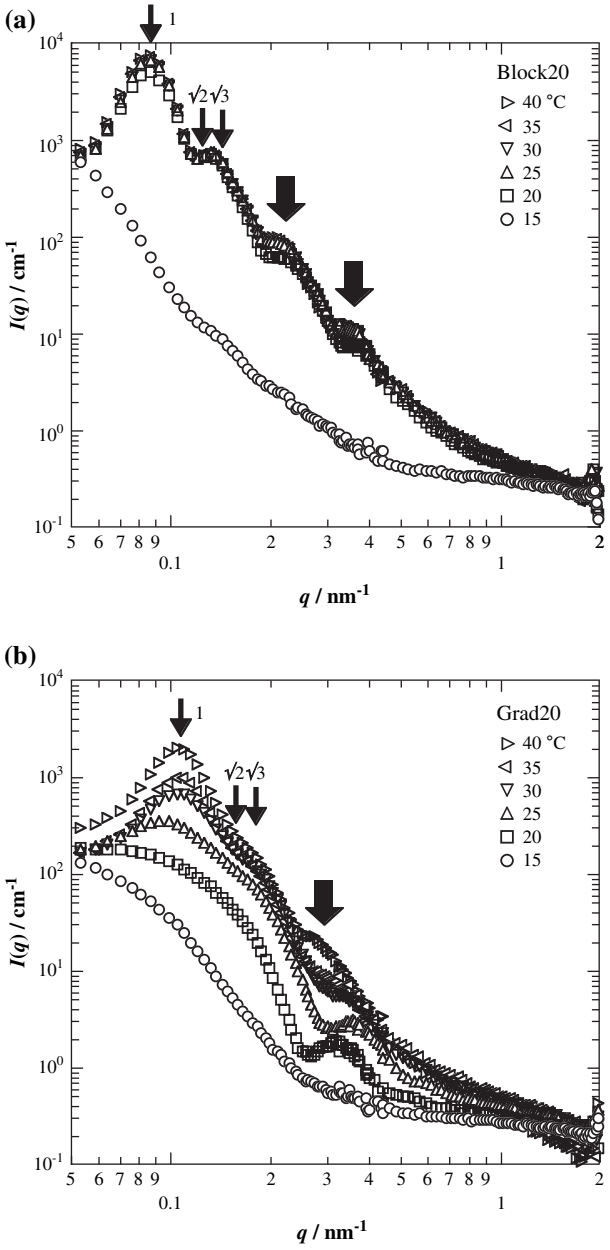

Fig. 3. SANS intensity functions (a) for Block20 and (b) for Grad20.

transitions were observed both for G' and G'' at 20 °C. These transitions indicate that the system becomes a physical gel above this temperature as was reported on a similar system [12,15]. On the other hand, Grad20 underwent a gradual and continuous transition. It is noteworthy that the temperature range, during which the system is a physical gel, is narrower than that of Block20, and the maximum value of G' in Grad20 is rather small by comparing with that in Block20. Interestingly, decreases in G' and G'' were observed at around 60 °C (indicated with a vertical line). This is due to precipitation as a result of dehydration of MOVE segments. The mechanism of physical gelation and the difference of the mechanical behavior in these systems will be elucidated in the following sections from the viewpoint of microscopic structures.

3.2. SANS

Fig. 3 shows the temperature dependence of the SANS intensity functions, $I(q)$s, for (a) Block20 and (b) Grad20. Here, q denotes the magnitude of the scattering vector. A detailed discussion on Block03 and Grad03, i.e., a discussion on single chain behavior, was made in the previous paper [9]. Let us focus here on the cases of Block20 and Grad20. Even at low T's (e.g., 15 °C), the microstructures of the two systems are different depending on the chemical architecture. Block20 has an upturn in $I(q)$ at low-q region, indicating interconnected micelles in addition to dispersed micelles, while Grad20 has a micelle-like independent particle scattering. By increasing T, more distinct differences between the systems became obvious. At 20 °C and higher T's, $I(q)$ for Block20 had several peaks as shown by arrows. This means that a microphase separation transition took place in the temperature range between 15 and 20 °C, and no further

structural change took place above this temperature. Note that the five SANS curves for $T \geq 20$ °C can be superimposed on each other (see Fig. 3a). On the other hand, Grad20 exhibits a gradual change in the SANS curves, indicating a gradual evolution of microdomain structures with respect to temperature.

These peaks can be assigned to the individual particle (thick arrows) and the inter-particle interference (thin arrows) since the system is apparently microphase-separated with a cubic lattice structure. It is expected that the interference is due to a body-centered cubic (bcc) macrolattice because the relative positions of the first, second, third peaks are 1, $\sqrt{2}$, $\sqrt{3}$ which are apparently distinguishable from the peak positions of 1, 2, 3 for lamella or liquid-like structures. In the case of Block20, a series of interference peaks (shown by the thin arrows) are clearly observed although the $\sqrt{2}$ and $\sqrt{3}$ peaks are indistinguishable by instrumental smearing effect. Different from the case of Block20, $I(q)$ for Grad20 changed continuously with T. At $T = 20$ °C, a particle scattering peak (thick arrow) without a significant inter-particle interference was observed. The particle scattering peak became broader and the interference peak (thin arrows) became sharper with increasing T. Hence, we can deduce that the structural transition, i.e., a macrolattice formation by way of an individual micelle formation, does occur in Grad20 though the transition is more gradual and the resulting structure is more indistinct than that of Block20.

In order to determine these structures, curve-fitting analyses were performed by assuming suitable models for the scattering contrast depending on the polymer concentration. Fig. 4 illustrates the scattering contrasts in (a) dilute and (b) semi-dilute solutions forming spherical micelles. In the case of Fig. 4a, micelles have a core-shell structure and are isolated by the solvent. On the other hand, in the case of Fig. 4b, micelles are densely packed in a macrolattice, resulting in only two phases, i.e., micelle core and the matrix (= a mixture of micelle corona and the solvent).

The scattering function for core-shell spheres is described elsewhere [9]. The scattering function for spherical particles with an inter-particle interference is described by the following equations:

$$I_{\text{particle}}(q) = nV^2\Delta\rho^2\Phi(qR_{\text{core}})^2Z(q) \tag{1}$$

$$V = \frac{4\pi R_{\text{core}}^3}{3} \tag{2}$$

$$\Phi(x) = 3\frac{\sin x - x\cos x}{x^3} \tag{3}$$

where n is the number of the spheres in a unit volume, R_{core} is the radius of the core, $\Delta\rho$ is the scattering length density difference between the sphere and the matrix, and $Z(q)$ is the lattice factor representing the interference of microdomains. In order to reproduce the scattering functions, a bcc lattice factor with paracrystallinity is introduced as described elsewhere [15–17]. Here, the instrumental smearing effect was also considered by introducing the resolution function which is related to the finite slit size and the wavelength distribution of the incident neutrons [15,18].

In addition to the scattering function for a macrolattice of spherical domains, an Ornstein–Zernike (OZ) function was introduced to reproduce the q^{-2} behavior at high-q region [16,19]. This function represents a homogeneous polymer solution as the matrix, i.e., the mixture of micelle corona and solvent:

$$I_{\text{matrix}}(q) = \frac{I_{\text{matrix}}(q=0)}{1+\xi^2q^2} \tag{4}$$

where ξ is the correlation length. The total scattering function is thus written as:

$$I(q) = I_{\text{particle}}(q) + I_{\text{matrix}}(q) \tag{5}$$

Note that this assumption neglects the detailed conformation of polymer chains near the micelle core–corona interface, which still nicely reproduces the microphase-separated structure of block copolymer solutions [16,19].

Prior to the curve fitting, the number density, n, was first determined from the first peak position, q_{max}, with the following equations:

$$n = \frac{2}{a^3} \tag{6}$$

$$a = \frac{2}{\sqrt{3}}\frac{2\pi}{q_{\text{max}}} \tag{7}$$

where a is the lattice constant of a bcc unit cell. The n values were evaluated to be 1.9×10^{15} cm^{-3} for Block20 at 40 °C and 3.9×10^{15} cm^{-3} for Grad20 at 40 °C, which were fixed during the curve fitting. Typical results of curve fitting are shown in Fig. 5. The dashed and thick lines denote the results without and with the OZ component, respectively. The estimated correlation length in the matrix $\xi = 1.0$ nm is reasonable and is in good agreement with that reported elsewhere [16]. The obtained parameters will be discussed below.

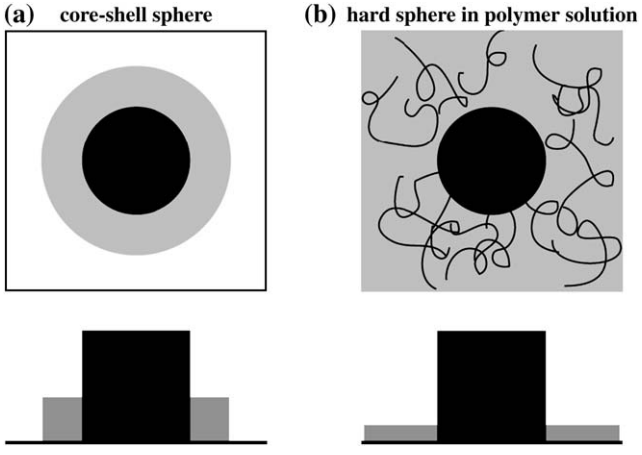

Fig. 4. Schemes of the micelle architecture and effective scattering contrast.

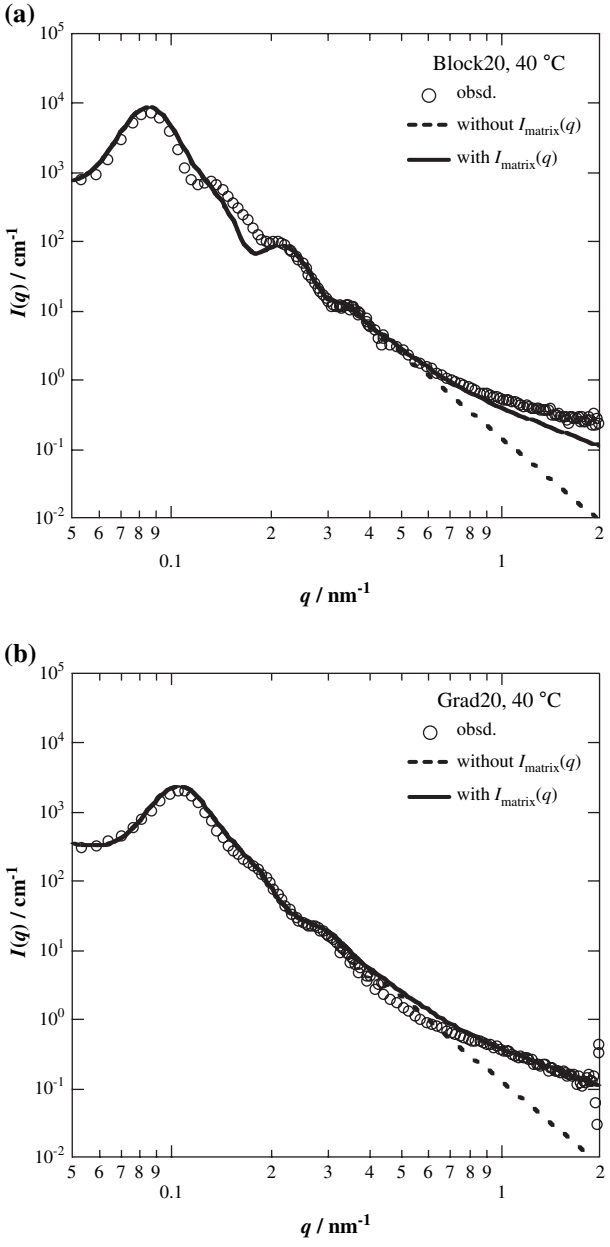

Fig. 5. Typical results of curve fitting by using the scattering function of hard spheres in a bcc paracrystal with a matrix of semi-dilute polymer solution.

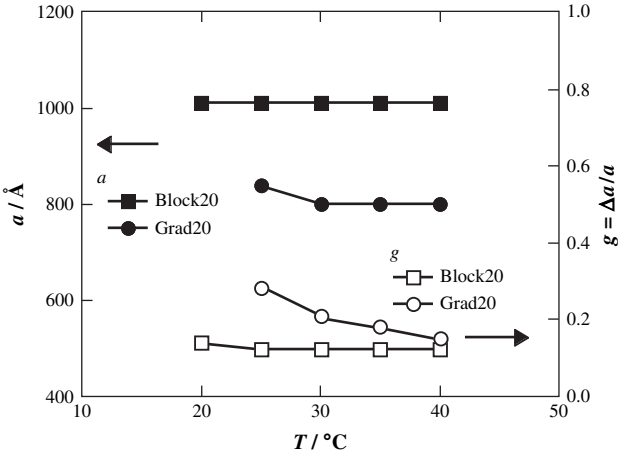

Fig. 6. Temperature variations of lattice constant, a, and the degree of paracrystallinity, g.

Fig. 6 shows the temperature variations of the paracrystal parameters. The lattice constant, a, is larger in Block20 than in Grad20. The difference in these values is almost of the same order of the diameter of the micelle cores in Block20 and in Grad20, i.e., 12–20 nm. On the other hand, the Hosemann's distortion factor, g [17], is dependent on T in Grad20 whereas it is rather constant in Block20. This is explained by the degree of interpenetration of the micelles as illustrated in Fig. 7. In the case of Block20, the interface of micelle core and corona is sharp and the inter-micelle distance is strictly optimized due to the deep potential [20]. In the case of Grad20, the micelles can be highly interpenetrated due to a broad boundary of the core–corona interface, allowing a larger fluctuation, i.e., larger g value. Hence, the physical gel of Grad20 is easier to flow, i.e., the gel region is narrower with respect to T, and G' is also smaller than that of Block20 (see Fig. 2b).

Fig. 8a shows the ratio of the scattering intensity from the particles to that from the matrix, $I_{particle}(q=0)/I_{matrix}(q=0)$, representing the relative contribution of the particle scattering. As clearly shown, the contribution of particle scattering is almost constant in Block20, whereas it is an increasing function of temperature in Grad20 with much smaller value than in Block20. This means that the microphase separation evolves in Grad20 with increasing temperature to form well-grown micelles. The temperature variations of the radii for micelle core, R_{core}'s, in Block and Grad systems are shown in Fig. 8b. For comparison, the R_{core} values for 0.3 wt% systems, i.e., Block03 and Grad03 [9], are also plotted in Fig. 8b as well as those for Block20 and Grad20. There are several interesting findings in this figure. (1) The value of R_{core} for Block20 is larger than that of Grad20, and independent of T, while R_{core} of Grad20 is an increasing function of T. (2) The value of R_{core} for Block20 is significantly larger than that of Block03. This is due to the fact that the size of spherical domains is an increasing function of the interaction parameter between polymer chain and solvent, resulting in the increase in the repulsive force enlarging the domain size. On the other hand, R_{core}'s for Grad20 and Grad03 are very similar both in the absolute values and in the T-dependence. The former means that Block has a larger interaction parameter between the core-chains and the solvent than that of Grad, and it is T-independent above the micellization transition temperature, T_{tr}. This fact again supports the "gradient" chemical architecture of Grad. The latter suggests that the micelle structures are the same in the two concentrations for Grad, but not for Block. Since the number of polymer chains forming a micelle is fixed for Block when microphase separation transition takes place, the value of R_{core} is T-independent for $T > T_{tr}$. On the other hand, that of Grad increases with T due to the "reel-in" effect. This reel-in phenomenon takes place not only in a dilute solution but also in a concentrated solution.

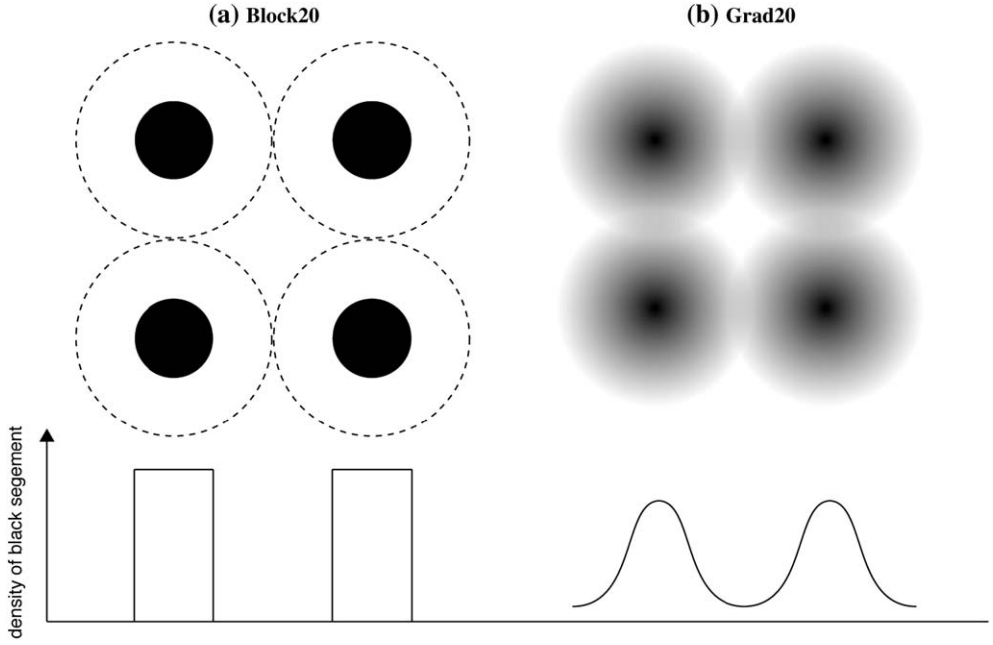

Fig. 7. Schematic illustrations for inter-micelle interaction (a) in Block20 and (b) in Grad20.

3.3. Mechanism of the formation of microphase separation

Fig. 9 shows the temperature variations of the scattering contrast, i.e., the scattering length density difference between the micelle core and matrix, $|\Delta\rho|$, for Block20 and Grad20 evaluated by the curve fitting. As clearly shown, $|\Delta\rho|$ in Block20 (solid squares) is constant with respect to T and is much larger than that in Grad20 (solid circles), whereas $|\Delta\rho|$ in Grad20 increased continuously with increasing T. The observed $|\Delta\rho|$ is related to the volume fractions of MOVE in the core as follows:

$$\begin{aligned}|\Delta\rho| &\equiv |\rho_{\mathrm{core}} - \rho_{\mathrm{matrix}}| \\ &= |(\phi_{\mathrm{core,EOVE}}\rho_{\mathrm{EOVE}} + \phi_{\mathrm{core,MOVE}}\rho_{\mathrm{MOVE}} + \phi_{\mathrm{core,D_2O}}\rho_{\mathrm{D_2O}}) \\ &\quad - (\phi_{\mathrm{matrix,EOVE}}\rho_{\mathrm{EOVE}} + \phi_{\mathrm{matrix,MOVE}}\rho_{\mathrm{MOVE}} + \phi_{\mathrm{matrix,D_2O}}\rho_{\mathrm{D_2O}})|\end{aligned} \tag{8}$$

with

$$\phi_{\mathrm{core,EOVE}} + \phi_{\mathrm{core,MOVE}} + \phi_{\mathrm{core,D_2O}} = 1 \tag{9}$$

$$\phi_{\mathrm{matrix,EOVE}} + \phi_{\mathrm{matrix,MOVE}} + \phi_{\mathrm{matrix,D_2O}} = 1 \tag{10}$$

where $\rho_{\mathrm{EOVE}} = 3.43 \times 10^{-7}$, $\rho_{\mathrm{MOVE}} = 4.39 \times 10^{-7}$, and $\rho_{\mathrm{D_2O}} = 6.34 \times 10^{-6}$ (Å^{-2}) are the scattering length densities of EOVE, MOVE, and D_2O, respectively, $\phi_{\mathrm{core,i}}$ is the volume fraction of the component i (= EOVE, MOVE or D_2O) in the micelle core, and $\phi_{\mathrm{matrix,j}}$ is the volume fraction of the component j (= EOVE, MOVE or D_2O) in the matrix. The dotted line in Fig. 9 indicates the perfect separation of Block20, i.e., the scattering length density difference between pure EOVE ($\phi_{\mathrm{core,EOVE}} = 1.0$) and the mixture of MOVE and D_2O, which is expressed as:

$$\begin{aligned}&|\Delta\rho_{\mathrm{perfect\ separation}}| \\ &\quad \equiv |\rho_{\mathrm{EOVE}} - (\phi_{\mathrm{matrix,MOVE}}\rho_{\mathrm{MOVE}} + \phi_{\mathrm{matrix,D_2O}}\rho_{\mathrm{D_2O}})|\end{aligned} \tag{11}$$

By assuming $\phi_{\mathrm{core,MOVE}} = \phi_{\mathrm{matrix,EOVE}} = 0$ and $\phi_{\mathrm{matrix,MOVE}} = 0.10$ ($=0.20 \times 0.5$) in Eq. (8), $\phi_{\mathrm{core,EOVE}}$ is evaluated for Block20, and thus the evaluated $\phi_{\mathrm{core,EOVE}}$ is plotted with open squares in Fig. 9. This means that ca. 40% of the volume in a micelle core is occupied by water molecules in Block20. The story is rather complicated in the Grad system because of the mixed nature of local monomer composition in a Grad polymer chain, i.e., $\phi_{\mathrm{core,MOVE}} \neq 0$, $\phi_{\mathrm{matrix,EOVE}} \neq 0$, etc.

Now, let us relate the fraction of dehydrated segments, $\phi_{\mathrm{p,HPB}}$, to the instantaneous composition in a Grad polymer chain, $\phi_{\mathrm{p,MOVE}}$, shown in Fig. 1, by assuming a linear relationship between temperature and the relative length of the hydrophobic segments along a Grad polymer chain during dehydration process.

$$\phi_{\mathrm{p,HPB}}(T) = \phi_{\mathrm{p,MOVE}}(\tilde{N}) \tag{12}$$

$$T = T_{\mathrm{tr}} + (T'_{\mathrm{tr}} - T_{\mathrm{tr}})\tilde{N} \tag{13}$$

with

$$T_{\mathrm{tr}} = 15\,^{\circ}\mathrm{C},\ T'_{\mathrm{tr}} = 60\,^{\circ}\mathrm{C}$$

where T'_{tr} is the precipitation temperature of the system, and $\tilde{N}(\equiv N_{\mathrm{HPB}}/N_{\mathrm{total}})$ is the normalized length of the hydrophobic segments along a Grad polymer chain. Here, N_{HPB} and N_{total} are the lengths of the hydrophobic segments and the total

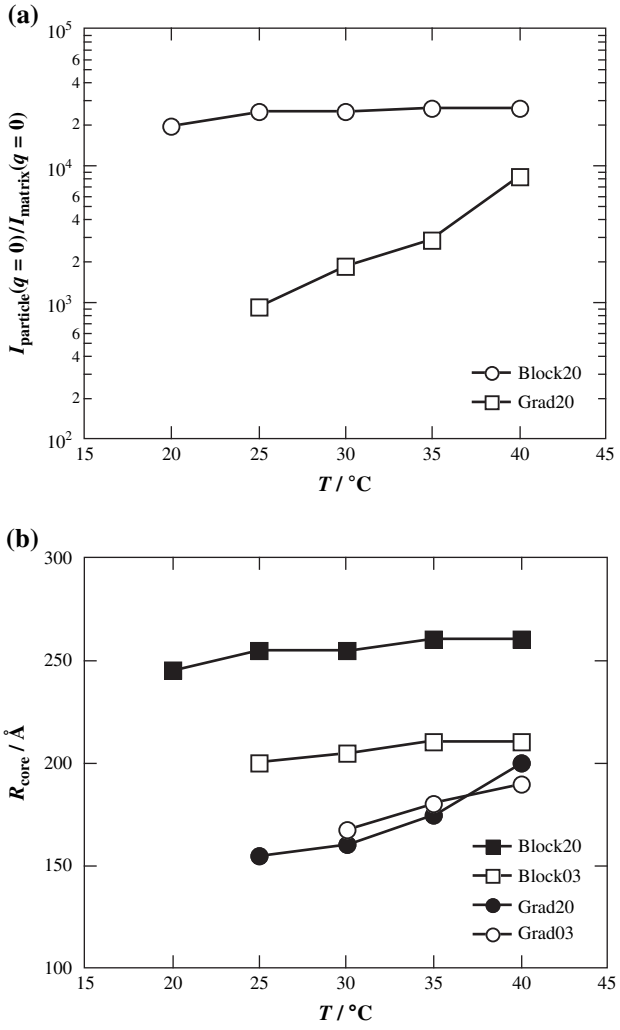

Fig. 8. Temperature variations (a) of the ratio of the scattering intensity from particle to that from the matrix, $I_{particle}(q = 0)/I_{matrix}(q = 0)$, and (b) of the core radius, R_{core}.

polymer chain, respectively. The volume fraction of the polymer chain in a micelle core, $\phi_{core,p}(T)$, can be calculated by:

$$\phi_{core,p}(T) = \phi_{p,HPB}(T)\phi_p \quad (14)$$

where ϕ_p is the volume fraction of Grad polymer chains in the solution, i.e., $\phi_p = 0.20$ for Grad20. The temperature dependence of the calculated $\phi_{core,p}(T)$ is shown by the broken line in Fig. 9, which is well correlated to that of the observed $|\Delta\rho|$. This means that the ''reel-in'' can be described by the instantaneous composition at polymer preparation, suggesting the possibility of precise controlling of the micelle structure by temperature. The present results are not affected by a thermal history and they are time-independent.

Lefebvre et al. predicted that a gradient in composition along the chain makes phase separation more difficult than for a block copolymer [5]. It is of interest to compare the strength of microphase separation between Block and Grad systems. Though the resulting structure in the present case is not lamellar but spherical, the combination of the micelle

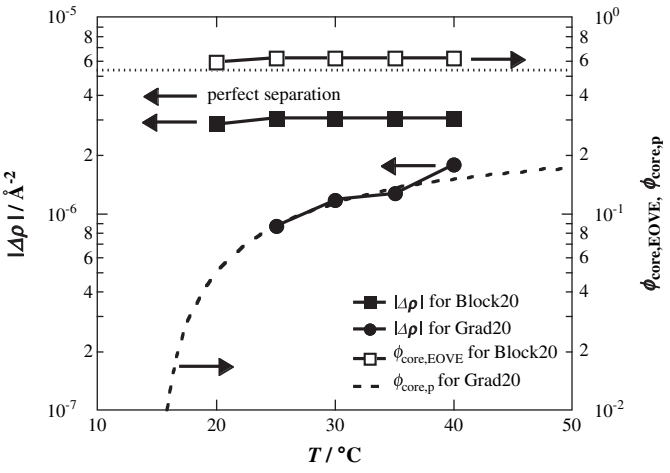

Fig. 9. Temperature variations of the scattering contrast factor, $|\Delta\rho|$ (solid symbols), and a perfect separation line representing $|\Delta\rho|$ for pure EOVE core in a mixture of MOVE and D_2O (dotted line). The calculated volume fractions of the polymer chains in a micelle core, $\phi_{core,EOVE}$ (for Block20, open squares) and $\phi_{core,p}$ (for Grad20, dashed line) are also plotted.

size and scattering contrast clearly shows the difference in the strength of microphase separation. That is, the stronger segregation of Block polymers causes larger micelles with smaller water content, whereas weaker segregation of Grad polymers causes smaller micelles with larger water content. In addition to the micelle architectures, the microphase-separated structure, i.e., the paracrystal parameters showed the effect of introducing gradient composition experimentally as the broadness of transition with respect to T.

4. Conclusion

The microdomain structures and the mechanism of microphase separation of gradient copolymer in water were investigated in terms of small-angle neutron scattering (SANS). The copolymers investigated here were p(EOVE$_m$-*grad*-MOVE$_n$)$_{m+n=600}$ (Grad) and pEOVE$_{300}$-*block*-pMOVE$_{300}$ (Block). Both EOVE and MOVE have lower critical solution temperatures in water at 20 and 65 °C. The chemical structure along Grad polymer chain varies rather linearly from pure EOVE to pure MOVE. Comparing with the Block copolymer consisting of pEOVE and pMOVE connected by a chemical bonding, i.e., a stepwise change of the chemical composition at the chemical bonding of EOVE and MOVE chains, the Grad copolymer exhibited a gradual structure formation and transition in addition to a gradual change in mechanical properties. The SANS investigations disclosed the following facts. (1) Micelle formation and microphase separation were observed both in block and gradient copolymer systems. (2) The microdomain structure of Grad is less ordered than that of Block due to the gradient chemical composition along the polymer chain. This may be one of the reasons why the storage and loss moduli vary gradually with temperature. (3) The resulting micelle size of Block was constant with respect to temperature, whereas that of Grad increased gradually with temperature. The latter is accounted for the ''reel-in'' effect

in micelle formation and microphase separation. (4) The sizes of micelle cores are nearly the same both in Grad03 and Grad20, whereas those in Block systems are significantly different. This difference is interpreted with the temperature-dependent composition of the domains exclusively in the case of Grad, that is, the radius and the volume fraction of the core are increasing functions of temperature. (5) The temperature variation of the scattering contrast is satisfactorily explained with the instantaneous composition along the Grad polymer chain. It is demonstrated that gradient copolymers have a potential applications for environment-sensitive materials because of tunability of their microstructures and physical properties.

Acknowledgment

This work was partially supported by Ministry of Education, Science, Sports and Culture, Japan (Grant-in-Aid Nos. 14350493 and 16350120 to M.S.). SANS experiments were carried out under the approval of the Neutron Scattering Program, the Institute for Solid State Physics, the University of Tokyo (Proposal No. 05.259).

References

[1] Molau GE. In: Aggarwal SL, editor. New York: Plenum Press; 1970.
[2] Helfand E, Wasserman ZR. In: Goodman I, editor. New York: Applied Science; 1982.
[3] Hamley IW. The physics of block copolymers. Oxford: Oxford University Press; 1998.
[4] Hashimoto H, Tsukahara Y, Tachi K, Kawai H. Macromolecules 1983; 16:648–57.
[5] Lefebvre MD, Olvera de la Cruz M, Shull KR. Macromolecules 2004;37: 1118–23.
[6] Aksimentiev A, Holyst R. J Chem Phys 1999;111(5):2329.
[7] Aoshima S, Sugihara S, Shibayama M, Kanaoka S. Macromol Symp 2004;215:151–63.
[8] Tsujimoto I, Aoshima S. Polym Prepr Jpn 2002;51:194.
[9] Okabe S, Seno K, Kanaoka S, Aoshima S, Shibayama M. Macromolecules 2006;39:1592–7.
[10] Mayo RF, Lewis MF. J Am Chem Soc 1944;66:1594–601.
[11] Aoshima S, Oda H, Kobayashi E. J Polym Sci Part A Polym Chem 1992; 30:2407.
[12] Okabe S, Sugihara S, Aoshima S, Shibayama M. Macromolecules 2003; 36:4099–106.
[13] Okabe S, Nagao M, Karino T, Watanabe S, Adachi T, Shimizu H, et al. J Appl Crystallogr 2005;38:1035–7.
[14] Shibayama M, Nagao M, Okabe S, Karino T. J Phys Soc Jpn 2005;74: 2728–36.
[15] Okabe S, Sugihara S, Aoshima S, Shibayama M. Macromolecules 2002; 35:8139–46.
[16] Fuse C, Okabe S, Sugihara S, Aoshima S, Shibayama M. Macromolecules 2004;37(20):7791–8.
[17] Hosemann R, Bagchi SN. Direct analysis of diffraction by matter. Amsterdam: North-Holland; 1962.
[18] Shibayama M, Okabe S, Nagao M, Sugihara S, Aoshima S, Harada T, et al. Macromol Res 2002;44:311.
[19] Dingenouts N, Norhausen C, Ballauff M. Macromolecules 1998;31: 8912.
[20] Whitmore MD, Noolandi J. J Chem Phys 1990;93:2946.